Conformational Analysis of *n*-Butane in Zeolite NaCaA: Temperature and Concentration Dependence†

Sanjoy Bandyopadhyay‡ and Subramanian Yashonath*,‡,§

Solid State and Structural Chemistry Unit and Supercomputer Education and Research Centre, Indian Institute of Science, Bangalore-560012, India

Received: October 30, 1996; In Final Form: May 14, 1997⊗

Investigations on *n*-butane sorbed in zeolite NaCaA have been carried out at several temperatures and sorbate concentrations in order to obtain the conformational properties. The configurational-bias Monte Carlo method has been employed. Results are compared with pure or unconfined fluid at the same density as the confined fluid. This provides insight into the role of the host on the conformational properties of *n*-butane. Surprisingly, unlike what is observed in silicalite or faujasite, the influence of zeolite on *n*-butane conformation is dependent on sorbate concentration. Effect of zeolite A is to decrease *gauche* conformer population at low sorbate concentrations and enhance it at high sorbate concentrations as compared to pure or unconfined fluid at the same density. It is shown that the conformational properties of *n*-butane in zeolite A are determined largely by the proximity of *n*-butane to the inner surface of α-cage and that steric factors have a relatively minor role. This is in contrast to silicalite where it is known that the steric factors play a major role. Such a proximity necessitates the curvature of the *n*-butane to be similar to that of the inner surface of the α-cage resulting in an enhancement of *gauche* conformer population. It is shown that sorbate−zeolite as well as sorbate−sorbate dispersion interactions are responsible for the proximity of the *n*-butane to the inner surface of the α-cage. Absence of sorbate−zeolite dispersion interactions gives rise to an increase in the *gauche* conformer population. The radial distribution function suggests that the confined fluid is more structured than the pure fluid at the same density indicating the strong influence the host has on the fluid structure.

1. Introduction

Alkanes are important organic molecules for several reasons. Firstly they play an all important role in petrochemical industries and are the predominant components in automobile, air, and cooking fuel. Long chain alkanes may be considered to be akin to polymers, and their study from this angle serves to yield insight into polymers. Zeolites, on the other hand, are important inorganic materials. They have excellent catalytic as well as separation properties.[1] They crystallize in a rich variety of structures, each quite different from the others, and a study of this variety is in itself interesting and important to inorganic chemists.[2] Alkanes in zeolites are important for plastic and petrochemical industries, and understading the interaction between them provides many challenges. For example, Karger and Ruthven[3] find that the nature of diffusion of alkanes in zeolites is actually quite complex. Experimental investigations into alkanes adsorbed in the pores of zeolites are innumerable, but yet our understanding is far from complete.[4−7] Even equilibrium properties of adsorbed alkanes in zeolites have not been understood well, in part, because of the many difficulties involved in making experimental measurements. Computer simulation provides an alternative technique that is both powerful and flexible to study these materials. In fact, during the past few years several workers have carried out simulation studies of alkanes in zeolites.[8−13]

Understanding conformation of alkanes in zeolites is important for gaining insight into equilibrium as well as dynamical properties. It is not clear what role the zeolite plays in determining the conformational equilibrium of alkanes. It would be interesting to investigate the various factors that influence the conformational properties and to clearly understand the way they influence the conformation. Here we report a study of *n*-butane in zeolite NaCaA. Our aim is to obtain the conformation of confined alkanes in this zeolite and further, to delineate the factors responsible for the observed behavior of the alkanes confined in zeolite NaCaA and, if possible, draw conclusions on other zeolites. The only technique that seems to provide reliable information about the conformation of chain molecules seems to be configurational bias Monte Carlo (CBMC). All results presented here have been obtained from this technique proposed recently by Smit and Siepmann.[14]

2. Methodologies

2.1. Structure of Zeolite A. The crystal structure of Linde 4A zeolite reported in the literature[15] has been employed in the present work. One unit cell of zeolite A has a composition $Na_{32}Ca_{32}Si_{96}Al_{96}O_{384}$. It belongs to the cubic space group $Fm\bar{3}c$ with lattice parameter $a = 24.555$ Å. Zeolite A consists of sodalite and α-cages or supercages. The sodalite cages have much smaller openings, and the alkane molecules are unable to enter these cages. There are in all eight α-cages in one unit cell of zeolite A. The approximate diameter of each α-cage is about 11.4 Å.[1,15] The α-cages are interconnected in an octahedral fashion via eight-ring windows of diameter 4.5 Å (see Figure 1). The sodium and calcium atoms occupy positions close to the center of the six-ring windows.

2.2. The Potential Model. *n*-Butane has been modeled in terms of united-atom interaction sites or beads, i.e., methyl (CH_3) and methylene (CH_2) groups are represented as single interaction centers, the site of interaction coinciding with position of the C atom. The distance between these interaction sites is the same as that of the C−C bond lengths, viz., 1.53 Å. This model has been found to be sucessful in modeling liquid *n*-butane.[14,16,17]

† Contribution No. 1259 from the Solid State and Structural Chemistry Unit.
‡ Solid State and Structural Chemistry Unit.
§ Supercomputer Education and Research Centre.
⊗ Abstract published in *Advance ACS Abstracts,* July 1, 1997.

S1089-5647(96)03379-2 CCC: $14.00

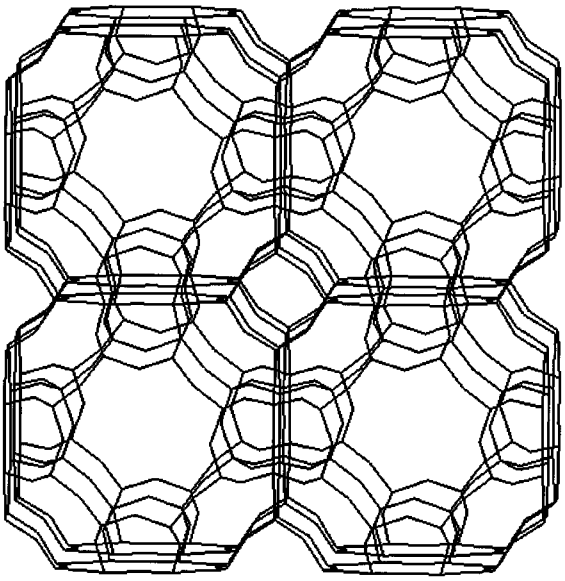

Figure 1. Topology of the eight α-cages of zeolite NaCaA. The α-cages have an approximate diameter of 11.4 Å and are interconnected in an octahedral fashion via eight-ring windows of diameter 4.5 Å.

Bond bending interactions between three adjacent sites are modeled in terms of a harmonic potential[18]

$$\phi_b(\theta) = \frac{1}{2}k_\theta (\theta - \theta_0)^2 \tag{1}$$

where θ_0 is the equilibrium bond angle and k_θ is the force constant. The values of θ_0 and k_θ are 114° and 6.25×10^4 K rad^{-2}, respectively. A torsional potential, governing rotation about nonterminal bonds is expressed in terms of a model proposed by Jorgensen[19]

$$\phi_t(\phi) = a_1(1 + \cos\phi) + a_2(1 - \cos(2\phi)) + a_3(1 + \cos(3\phi)) \tag{2}$$

with $a_1 = 355.03$ K, $a_2 = -68.19$ K, and $a_3 = 791.32$ K.

The intermolecular site−site interactions between *n*-butane molecules are modeled in terms of the united-atom model consisting of site−site pairwise interactions of the (12-6) Lennard-Jones form given by

$$\phi_{ss}(r_{ss}) = 4\epsilon_{ss}\left[\left(\frac{\sigma_{ss}}{r_{ss}}\right)^{12} - \left(\frac{\sigma_{ss}}{r_{ss}}\right)^{6}\right] \tag{3}$$

The self-interaction parameters used in the present study are $\sigma_{CH_3} = \sigma_{CH_2} = 3.93$ Å, $\epsilon_{CH_3} = 114$ K, and $\epsilon_{CH_2} = 47$ K. These parameters were taken from the work of Smit and Siepmann.[14] The cross-interaction parameters between CH_3 and CH_2 groups are obtained from the well-known Lorentz−Berthelot combination rules.[20]

The sorbate−zeolite interactions $\phi_{sz}(r_{sz})$ are also modeled in terms of pairwise (12-6) Lennard-Jones form

$$\phi_{sz}(r_{sz}) = 4\epsilon_{sz}\left[\left(\frac{\sigma_{sz}}{r_{sz}}\right)^{12} - \left(\frac{\sigma_{sz}}{r_{sz}}\right)^{6}\right] \tag{4}$$

with interaction parameters σ_{sz} and ϵ_{sz}, between the united-atoms $s = CH_3$ or CH_2 and zeolite atoms z = O, Na, Ca. Interactions between the sorbate molecule and the framework Si/Al atoms are not included since the close approach of the sorbates is prevented by the surrounding bulkier oxygens. The self-interaction parameters of the zeolite atoms used in this study are $\sigma_O = 2.79$ Å, $\sigma_{Na} = 3.26$ Å, $\sigma_{Ca} = 3.35$ Å, $\epsilon_O = 211.8$ K, $\epsilon_{Na} = 10.7$ K, $\epsilon_{Ca} = 1148.1$ K.[21] The cross-interaction parameters between *n*-butane and the zeolite atoms obtained using the combination rules[20] are listed in Table 1. The dispersion and the repulsive interaction terms between the sorbate and the zeolite atom are given by $A_{sz} = 4\epsilon_{sz}\sigma_{sz}^6$ and $B_{sz} = 4\epsilon_{sz}\sigma_{sz}^{12}$, respectively. The corresponding interaction energies for each of the above four types of interactions are obtained by summing over the contributions from individual molecules and their mutual interactions and interactions with the zeolite atoms. The total potential energy is therefore

TABLE 1: Potential Parameters for Sorbate−Zeolite Interactions

type	A_{sz} (10^3 kJ/(mol Å^6))	B_{sz} (10^6 kJ/(mol Å^{12}))
CH_3−O	7.4350	10.6983
CH_3−Na	2.5113	5.4284
CH_3−Ca	27.9843	65.0913
CH_2−O	4.7739	6.8693
CH_2−Na	1.6125	3.4855
CH_2−Ca	17.9685	41.7945

$$U_{tot} = U_b + U_t + U_{ss} + U_{sz} \tag{5}$$

Induction interactions between *n*-butane and the zeolite atoms are not included here. Earlier simulations of *n*-butane in zeolites have neglected the polarization term. In the present case, the presence of Na^+ and Ca^{2+} lead to non-negligible electrostatic field. However, the polarizibility α of a methyl group is smaller than that of Xe, and therefore one expects that this contribution will be less important in the present case. Usually, induction contributions are less than 1% and at best about 4% of the total interaction energy, and the computation of it is rather involved. Consequently, we decided to exclude these terms from the calculation.

2.3. Computational Details. Monte Carlo (MC) calculations were carried out in the canonical ensemble at fixed (*N*,*V*,*T*). Cubic periodic boundary conditions were employed.[20] An attempt is made to displace a molecule randomly, rotate it by a random amount around a randomly chosen axis, and, finally, to regrow either a part or all of it. *N* such attempts comprise a MC cycle during which the molecule itself is selected randomly. Attempt to regrow the molecules is carried out as proposed by Smit and Siepmann,[14] and the method is itself known as configurational-bias Monte Carlo (CBMC). Calculations have been performed on one unit cell of zeolite A which consists of eight α-cages. Simulations were carried out on 8 and 40 *n*-butane molecules corresponding to a sorbate concentration, c, of one and five *n*-butane molecules per α-cage. Simulations were carried out at three different temperatures of 200, 300, and 400 K at a low sorbate concentration of $c = 1$ *n*-butane/α-cage and at two different temperatures of 200 and 400 K at high sorbate concentration of $c = 5$ *n*-butanes/α-cage. Equilibration was performed over 2500 MC cycles. This is followed by production runs of 10^5 MC cycles at a loading of $c = 1$ *n*-butane per α-cage and 2.5×10^4 MC cycles at a loading of $c = 5$ *n*-butanes per α-cage to obtain averages of the properties. A spherical cut-off of 12 Å has been employed in evaluating both sorbate−sorbate and sorbate−zeolite interaction energies.

3. Results and Discussion

3.1. *n*-Butane Conformation. The average values of different interaction energies, such as, butane−butane or sorbate−sorbate interactions (U_{ss}), butane−zeolite or sorbate−zeolite interactions (U_{sz}), bond-bending interactions (U_b), torsional interactions (U_t), and the total interaction potential energy (U_{tot})

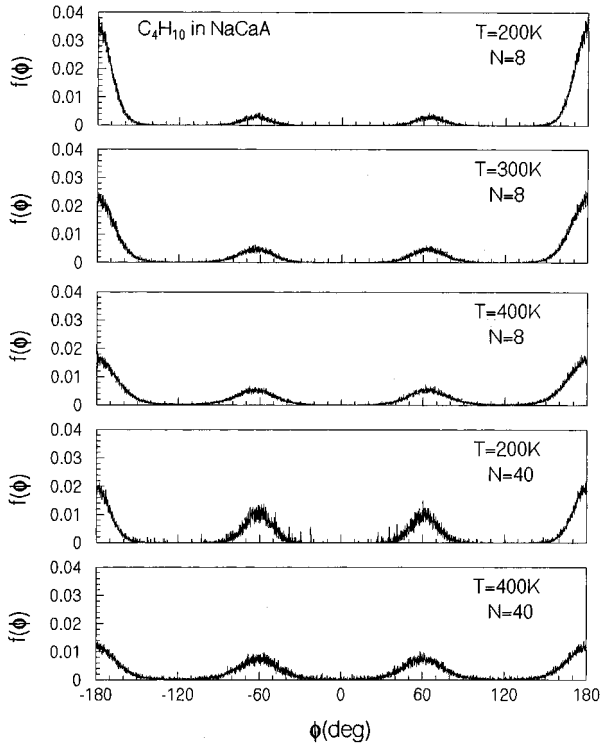

Figure 2. Dihedral angle distribution functions $f(\phi)$ for *n*-butane confined within the α-cages of zeolite NaCaA at different temperatures and concentrations.

TABLE 2: Equilibrium Thermodynamic Properties of *n*-Butane in Zeolite NaCaA at Different Temperatures and Concentrations

T (K)	N	U_{ss} (kJ/mol)	U_{sz} (kJ/mol)	U_b (kJ/mol)	U_t (kJ/mol)	U_{tot} (kJ/mol)	q_{st} (kJ/mol)
200	8	−1.01	−58.26	0.84	1.40	−57.03	58.69
300	8	−2.42	−53.59	1.24	2.47	−52.30	54.79
400	8	−1.45	−51.24	1.65	3.41	−47.63	50.96
200	40	−9.32	−53.81	0.86	2.75	−59.52	61.18
400	40	−7.83	−50.92	1.74	4.05	−52.96	56.29

as well as the isosteric heats of adsorption (q_{st}) at three different temperatures of 200, 300, and 400 K for a low concentration of one *n*-butane molecule per α-cage, and at two different temperatures of 200 and 400 K for a high concentration of five *n*-butane molecules per α-cage, are listed in Table 2. From the table it is clear that the sorbate−zeolite interaction energy is the predominant one, whereas the contributions from bond-bending interactions (U_b) and torsional interactions are rather small. The sorbate−sorbate interaction energy (U_{ss}) becomes quite significant at high sorbate concentrations. For a particular sorbate concentration, as the temperature is increased the interaction energies also increase. This trend is reflected in the isosteric heat of adsorption (q_{st}) values.

The dihedral angle distribution functions $f(\phi)$ for *n*-butane in zeolite A at different temperatures (200, 300, and 400 K) at a low sorbate concentration of $c = 1$ *n*-butane/α-cage and at temperatures of 200 and 400 K for a sorbate concentration $c = 5$ *n*-butane/α-cage are shown in Figure 2. From the figure it is clear that the *gauche* conformer population increases with temperature as one would expect. The percentages of the *trans* and *gauche* populations for the confined fluid at various sorbate concentrations and temperatures are listed in Table 3. The increase of bond-bending (U_b) and torsional interaction energies (U_t) with increase in temperature can be attributed to the increase in the population of *gauche* conformation.

In order to understand the influence of the zeolite on the conformational equilibrium of confined *n*-butane, one would like to have a standard against which comparison could be made. Earlier studies, notably that of Hernandez and Catlow, used ideal gas as the standard. However, at higher concentrations such as, for example, $c = 5$ *n*-butanes/α-cage, it would be more appropriate to compare with pure fluid at the corresponding density rather than the infinitely dilute ideal gas. This is what we shall do here. This we hope will unamibiguosly show the effect of confinement since all other factors such as temperature, density, etc. will be identical for the pure fluid as well as for the confined fluid. In order to do this, one needs to estimate the volumes of the α-cages which we do so by a method we have recently proposed.[22,23] Estimate of the α-cage volume leads to a density of $\rho = 0.1534$ g/cm^3 for $c = 1$ *n*-butane/α-cage and $\rho = 0.7670$ g/cm^3 for $c = 5$ *n*-butanes/α-cage. Calculations on pure *n*-butane have been carried out at these densities.

TABLE 3: Relative Population of *trans* and *gauche* Forms of *n*-Butane in Zeolite NaCaA at Different Temperatures and Concentrations[a]

			confined fluid (cf)		pure fluid (pf)		d = % g(cf) − % g(pf)
T (K)	N	ρ (g/cm^3)	% *trans*	% *gauche*	% *trans*	% *gauche*	
200	8	0.1534	85.1	14.9	81.5	18.5	−3.6
400	8	0.1534	59.6	40.4	58.1	41.9	−1.5
200	40	0.7670	48.5	51.5	81.7	18.3	33.2
400	40	0.7670	43.3	56.7	50.2	49.8	6.9

[a] Populations of *gauche* form in ideal gas are 20 and 41.9% at 200 and 400 K, respectively.

The relative population of *trans*/*gauche* forms for pure *n*-butane at these estimated densities are listed in Table 3. First is a comparison of the results for pure fluid with those for ideal gas: at low sorbate density (0.1543 g/cm^3) the populations of *gauche* conformers is 41.9% and 18.5%, respectively, at 400 and 200 K, which are rather close to the ideal gas values (41.9% and 20%). At $\rho = 0.7670$ g/cm^3 and 400 K, the values for pure fluid and ideal gas are quite different: 49.8% and 41.9%, respectively. Clearly, the relative populations of *trans* and *gauche* forms in pure fluid at high densities deviate significantly from the ideal gas values. Therefore, it is important to make comparison with the pure fluid rather than the ideal gas. This way we will be able to isolate the effect of confinement alone from other factors such as density, temperature, etc. The difference, d, between the *gauche* conformer population of the confined fluid and the pure fluid is listed in Table 3. It is interesting to compare the *gauche* populations in these two systems:

(1) At *low sorbate concentrations, viz.*, $\rho = 0.1534$ g/cm^3, the *gauche* population is lower in confined fluid at all temperatures.

(2) At *high sorbate concentrations, viz.*, $\rho = 0.7670$ g/cm^3, the *gauche* population is higher in confined fluid at all temperatures as compared to the pure fluid at the respective density.

The difference, d, is particularly significant at low temperature and high sorbate concentration (33.2%).

Studies of *n*-butane adsorbed in silicalite by Hernandez and Catlow[17] have indicated that a significant enhancement of *trans* conformer population occurs in the confined fluid (e.g., 70% at 400 K) as compared to ideal gas (e.g., 60% at 400 K) at all concentrations and temperatures studied by them. Theodorou and co-workers also observed similar trends.[24] Recent investigations on *n*-butane in zeolite Y by us[22] indicated an enhancement in *gauche* conformer population at all temperatures and concentrations. The results obtained by us here for zeolite A differ from all these in that there is enhancement of *trans*

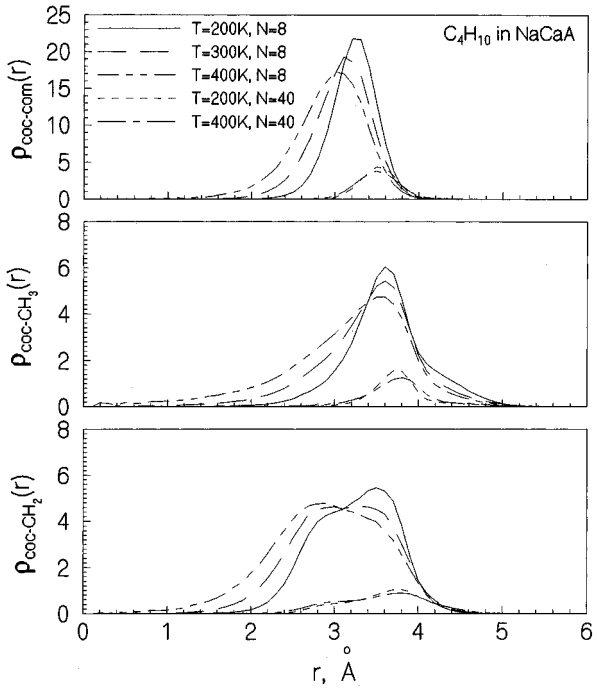

Figure 3. Single particle radial distribution functions ($\rho_{coc-com}$, ρ_{coc-CH_3}, ρ_{coc-CH_2}) of the center-of-mass (com), CH_3, and CH_2 groups of the *n*-butane molecules as a function of the distance, *r*, from the center of the α-cage (coc), at different temperatures and sorbate concentrations. A *n*-butane molecule is considered to reside in an α-cage if the distance (*r*) of its com to that cage center is the shortest among the distances of the com with all cage centers.

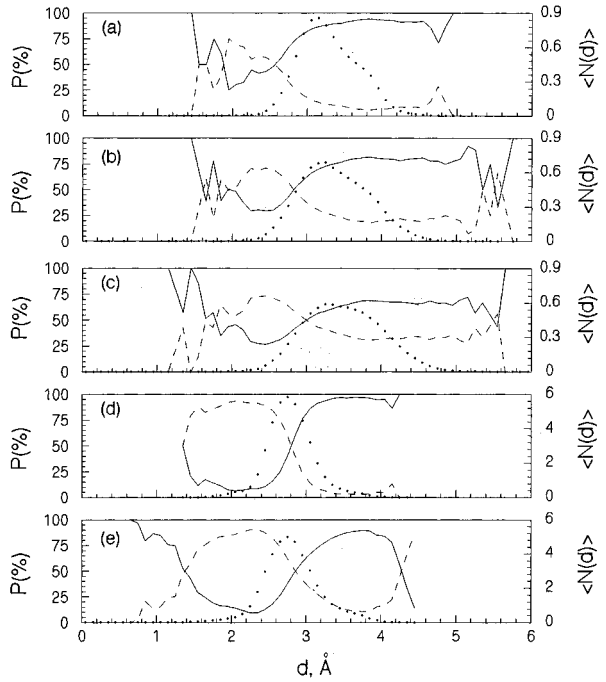

Figure 4. Percentage variation of *trans* /*gauche* population as a function of distance *d* from the plane of the window. The shortest among the six distances of the com of a *n*-butane molecule from the six window planes of an α-cage in which the molecule resides is taken as the value for *d*. The continuous curve corresponds to the *trans* form and the dashed curve corresponds to the *gauche* form. The dotted line shows the probability of finding *n*-butane molecules from the plane of the window. (a) $T = 200$ K, $c = 1$ *n*-butane/α-cage; (b) $T = 300$ K, $c = 1$ *n*-butane/α-cage; (c) $T = 400$ K, $c = 1$ *n*-butane/α-cage; (d) $T = 200$ K, $c = 5$ *n*-butanes/α-cage; (e) $T = 400$ K, $c = 5$ *n*-butanes/α-cage.

under certain conditions and of *gauche* under other conditions. One other difference may be noted: the dihedral angle distribution function, $f(\phi)$, shows an increase in intensity in the region intermediate between those of *trans* and *gauche*, i.e., between $\phi = 60$ and 180° in the case of silicalite which we do not find in the present case. In view of the larger volume of the α-cage we would have expected that conformation intermediate between the *trans* and *gauche* would be more prevalent in zeolite A. Earlier studies on adsorption of small molecules such as xenon, methane, etc. indicated that several factors could influence their diffusion properties. In particular the sorbate−zeolite interaction played an important role in giving rise to the levitation effect.[25,26] In order to understand the possible reasons for the behavior exhibited by *n*-butane in zeolite A described above, we have carried out detailed analysis, which is given below.

3.2. Relationship between Conformation and Location within the Cage. The single particle radial distributions $\rho_{coc-com}(r)$ of the center-of-mass (com) of the *n*-butane molecules from the center of the cage (coc) are shown in Figure 3 at all temperatures and concentrations. This distribution function is defined as

$$\rho_{coc-com}(r) = \frac{\langle n(r) \rangle}{4\pi r^2 \, dr \, \rho_b} \tag{6}$$

where $\langle n(r) \rangle$ is the average number of sorbate molecules between r and $r + dr$ from the cage center, ρ_b is the bulk density of the confined fluid. Here r is the distance of the center-of-mass of the *n*-butane molecule from the center of the cage in which it is resident. A given molecule of *n*-butane is said to be resident in a cage if the distance from its com to that cage center is the shortest among the set of distances of the com with all cage centers.[21]

It is generally observed that the population of the molecules near the cage center is almost zero at all concentrations and temperatures, which shows that the molecules have a preference for the region near the inner surface of the cage. This is quite similar to that observed for argon in zeolite A and methane and xenon in zeolite Y.[10,21,27] The temperature dependence of $\rho_{coc-com}(r)$ of *n*-butane in zeolite A is also found to be similar to that exhibited by argon in A, methane and xenon in Y, viz., the sorbates increasingly occupy regions near the cage center as the temperature is increased. In contrast to this, the concentration dependence of $\rho_{coc-com}(r)$ is quite different. In the case of other guests, it was found that with increase in concentration, $\rho_{coc-com}(r)$ the peak width increased and further there was a gain in intensity near the cage center. In the present study we find that the peak has a lower width at higher concentrations and further the peak shifts from 3 Å at $c = 1$ *n*-butane/α-cage to 3.5 Å at $c = 5$ *n*-butanes/α-cage. Table 2 lists the U_{ss} at various temperatures as the concentration is increased from 1 to 5 *n*-butanes/α-cage. U_{ss} makes a significant gain with increase in sorbate concentration. In comparison the change of U_{sz} is rather small. We attibute the lower half-width as well as the shift to higher values of r to stronger sorbate−sorbate interaction. Also shown in Figure 3 are the *coc*-CH_3 and *coc*-CH_2 distribution functions. The peaks have a much broader width. The CH_3 group exhibits a nonzero value of ρ even near $r = 0$ Å especially for $c = 1$ *n*-butane/α-cage. As we shall see this has implications about the conformation of the confined *n*-butanes at this concentration.

Figure 4 shows a plot of the percentage of *trans*/*gauche* conformer as a function of distance, *d*, from the window plane. The continuous curve corresponds to the *trans* form and the dashed line corresponds to the *gauche* form. The dotted line shows the probability, $\langle N(d) \rangle$, of finding *n*-butane molecules from the plane of the window. It is seen that probability of

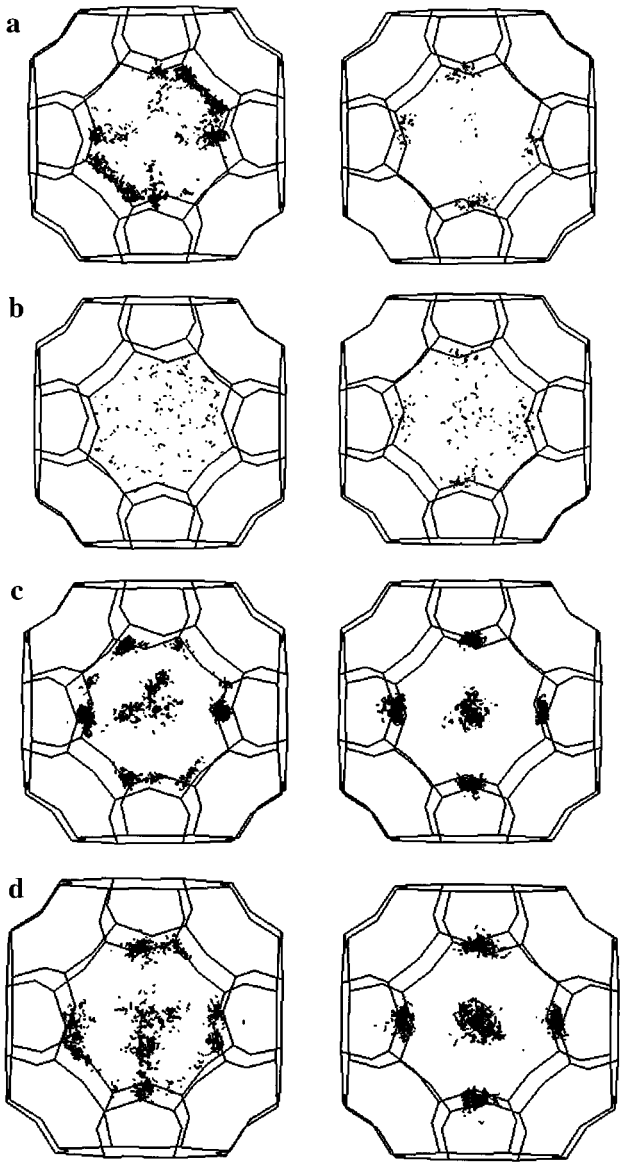

Figure 5. Density of center-of-mass position of the *trans* and *gauche* conformers within an α-cage of zeolite NaCaA obtained from the MC simulations at (a) $T = 200$ K, $c = 1$ *n*-butane/α-cage, (b) $T = 400$ K, $c = 1$ *n*-butane/α-cage, (c) $T = 200$ K, $c = 5$ *n*-butanes/α-cage, and (d) $T = 400$ K, $c = 5$ *n*-butanes/α-cage. Left cage gives *trans* conformer density while the right one gives the *gauche* conformer density. Note the stronger preference exhibited by the *gauche* to certain regions within the α-cage.

finding a *gauche* is rather small as compared to *trans* especially at 200 K and 1 *n*-butane/α-cage. As already seen this probability increases with increase in temperature and concentration. More importantly, the probability of finding a *gauche* at a distance of about 2 Å from the window plane of the eight-ring window is always found to be significantly higher than those at other *d* values.

Figure 5 shows an α-cage of zeolite A, along with the center-of-mass positions over several MC steps, of the *trans* and *gauche* conformers obtained from simulations at different temperatures and sorbate concentrations. It is evident from this figure that *gauche* conformers occupy regions in the α-cage which are different from those of *trans*. This suggests that there is a relationship between the conformation and the position of the molecule within the α-cage. It is worth noting that the *gauche* *n*-butane is highly specific with regard to the positions it occupies inside the cage while *trans* conformer exhibits less of such preference. The *gauche* conformer prefers the site in front

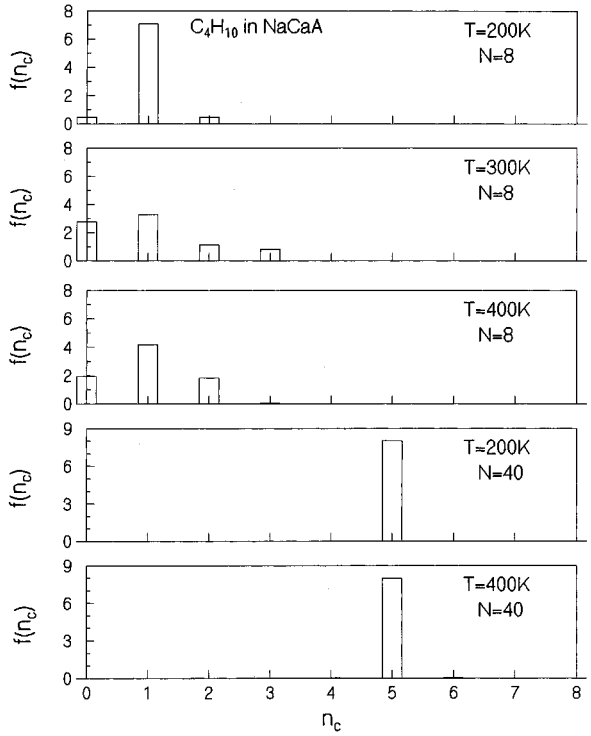

Figure 6. Distribution of the α-cage occupancy $f(n_c)$ at different temperatures and sorbate concentrations. Note that, there appears to be diffusion from one cage to another, although small, at low sorbate concentration of $c = 1$ *n*-butane/α-cage, whereas at high sorbate concentration of $c = 5$ *n*-butanes/α-cage, there is no such diffusion leading to a single peak at $n_c = 5$.

of the eight-ring window. There are six such windows, and *gauche* can be found in front of each of these windows. This is consistent with Figure 4 where we find that the probability of finding *gauche* was higher near 2 Å from the window plane. This increased probability of *gauche* in Figure 4 corresponds to the region shown in Figure 5. Figure 6 shows the distribution of cage occupancy $f(n_c)$ at different temperatures and sorbate concentrations. At a low sorbate concentration of $c = 1$ *n*-butane/α-cage, there appears to be diffusion from one cage to another though still small. The presence of a single peak in the distribution at $c = 5$ *n*-butanes/α-cage suggests the absence of diffusion. Even at low concentration, the diffusion from one cage to another is not facile. At high concentration, the strong sorbate−sorbate interactions in *n*-butanes make it even more difficult. As we shall see below, sorbate−sorbate interactions also play an important role in determining several other properties.

3.3. Effect of Concentration on *n*-Butane Conformation. As the sorbate concentration is increased from one to five *n*-butanes/α-cage the *gauche* population increases from 14.9% to 51.5% at 200 K and from 40.4% to 56.7% at 400 K. The increase at 200 K is 36.6%, which is rather large. The increase in *gauche* population is much smaller at 400 K, where the change is 16.3%. A much smaller increase of *gauche* population with concentration is observed in silicalite by Hernandez and Catlow:[17] 9.3% to 11.5% or just 2.2% when the sorbate concentration changes from two to eight *n*-butanes/unit cell at 300 K. In pure *n*-butane the *gauche* population remains almost unchanged at low temperature (200 K) when the sorbate concentration is increased from one to five *n*-butanes/α-cage. But at 400 K the *gauche* population increases by almost 8% in pure fluid. It is evident that a much larger increase in *gauche* population is observed in the case of fluid confined in zeolite A.

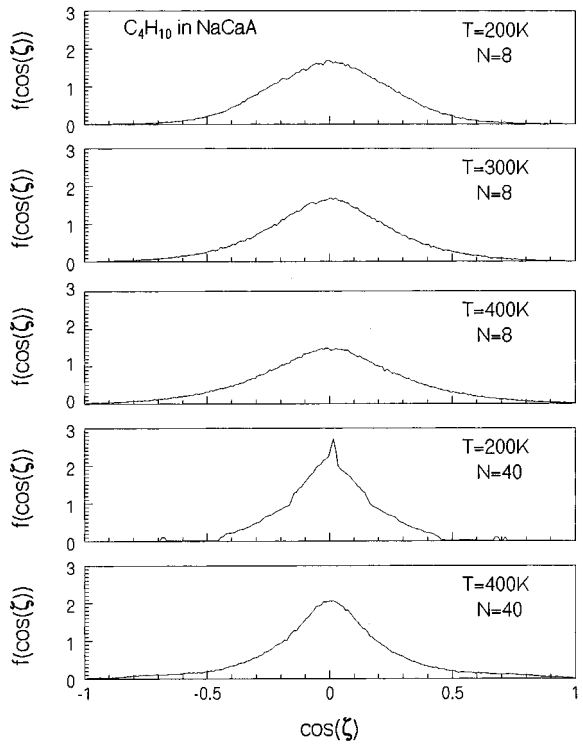

Figure 7. Distribution of cos ζ between the end-to-end vector **R** and the vector $\mathbf{r}_{coc-com}$ from the center of the α-cage where the *n*-butane molecule is resident to the center-of-mass (com) of the *n*-butane molecule at different temperatures and concentrations. It is clear from the figure that the distribution peaks around $\zeta = 90°$ (cos $\zeta = 0$) under all conditions indicating a preference of *n*-butanes to remain parallel to the inner surface of the α-cage.

The differences in the conformer populations between fluid confined in zeolite A on the one hand and silicalite and zeolite Y as well as the pure fluid on the other indicate that the zeolite—or in general the host—exerts influence on the conformation of *n*-butanes in different ways. In the case of silicalite the rather narrow and straight or sinusoidal channels are likely to favor a *trans* conformation rather than a *gauche* conformation. Thus, while in silicalite the conformational equilibrium is determined by the steric factors and arises from the shape of the channel vis-a-vis that of the *trans* and *gauche* conformers, the large cages in zeolite A offer no explanation regarding the difference in the conformer population between the confined and the pure fluid. In order to obtain some insight into what might be happening, we first take a look at 200 K and $c = 5$ *n*-butanes/α-cage, where the *gauche* conformer population deviates to the maximum from that of the pure fluid. From Figure 3, which shows the distribution of the com positions of the *n*-butane, it is clear that the position of the maximum is at around 3.5 Å, which is higher than at any other temperature or sorbate concentration. In the case of smaller molecules such as argon, it was found that the peak occurred[21] around 4.0 Å, but this difference of about 0.5 Å may be attributed to the difference in their sizes. Figure 7 displays the distribution f(cos ζ), where ζ is the angle between the end-to-end vector **R** and the vector $\mathbf{r}_{coc-com}$ from the cage center to the center of mass of the *n*-butane

$$\cos \zeta = \frac{\mathbf{R}\cdot\mathbf{r}_{coc-com}}{|\mathbf{R}||\mathbf{r}_{coc-com}|} \qquad (7)$$

$\zeta = 0°$ corresponds roughly to a molecule that is perpendicular to the inner surface, whereas $\zeta = 90°$ corresponds to the orientation of the *n*-butane in which it is, roughly speaking,

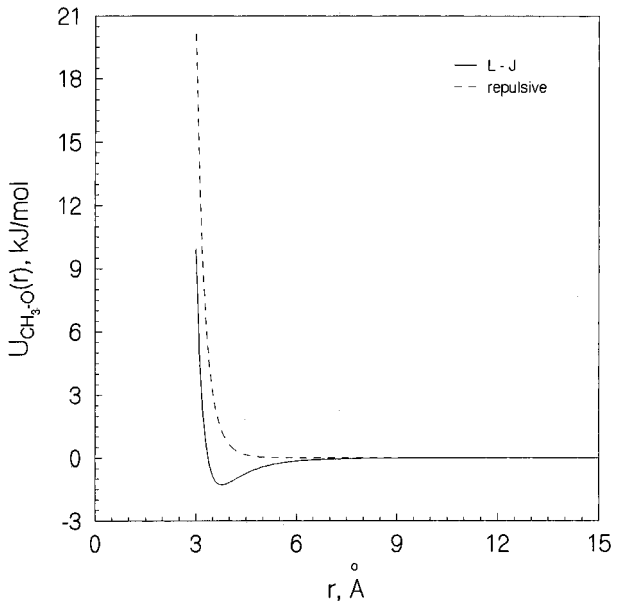

Figure 8. Comparison of the Lennard-Jones potential energy of interaction and pure repulsive form ($1/r^{12}$) between a CH_3 group and oxygen atoms. Note the presence of a relatively long tail with positive energies in the absence of the dispersion term leading to a reduction in the α-cage radius.

"parallel" to the inner surface of the α-cage. It is seen that the distribution peaks around $\zeta = 90°$ under all conditions indicating a predominance of *n*-butane which lie parallel to the inner surface. However, at low sorbate concentrations, the distribution is broad suggesting that *n*-butane can take other orientations as well. In particular, *n*-butanes now assume orientations which deviate significantly from the "parallel" orientation, such as, for example, $\zeta = 60°$, etc. Nonzero intensity near $r = 0$ Å, in the distribution $\rho_{coc-CH_3}(r)$ (Figure 3) supports this view. At $c = 5$ *n*-butanes/α-cage and particularly at 200 K, we find that the peak at $\zeta = 90°$ is relatively more intense and also has lower fwhm (full-width at half maximum). This suggests that the *n*-butanes are mostly "parallel" to the inner surface of the α-cage under these conditions. This coupled with the earlier observation that the peak in $\rho_{coc-com}(r)$ shifts from 3 to 3.5 Å indicates that the backbone of the *n*-butane molecules now runs along the inner wall of the cage. Therefore, it seems that the curvature of the inner wall of the α-cage essentially determines the conformer population by necessitating the curvature of the *n*-butane molecule to be the same as that of the inner wall of the α-cage. The curvature of the *gauche* conformer, which is boatlike, seems to better match the curvature of the α-cage rather than the chairlike *trans* conformer. The reason for the shift in the position of the peak in $\rho_{coc-com}(r)$ toward larger values of r seems to be, in part, due to the significant sorbate−sorbate interaction. From Table 2 we can see that U_{ss} is highest for 200 K and $c = 5$ *n*-butanes/α-cage and is about 20% of U_{tot}.

In order to verify the role of the sorbate−zeolite interaction, we carried out calculations in which we put the sorbate−zeolite dispersion interactions to zero. When the sorbate−zeolite dispersion term is absent, the cage volume decreases since the Lennard-Jones interaction potential now acquires a long repulsive tail as shown in Figure 8. This leads to a decrease in the available volume of the cage and as a consequence an increase in the curvature, κ, of the inner surface since $\kappa = 1/r$. So, while the absence of attraction between the *n*-butane and the zeolite wall is expected to lead to a decrease in *gauche* population, the increase in curvature is expected to lead to an increase in the *gauche* population if the *n*-butanes are unable to migrate from one cage to another. This is in fact the case for zeolite A. The

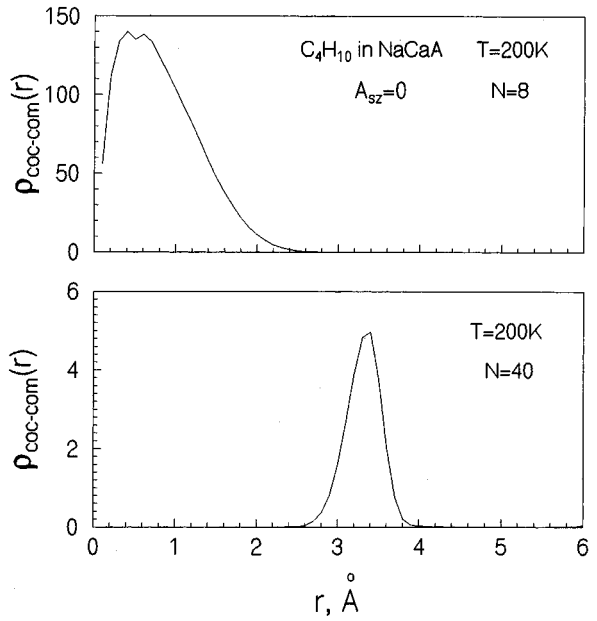

Figure 9. Single particle radial distribution function of the center-of-mass of *n*-butane molecules from the center of the α-cage $\rho_{coc-com}(r)$ in the absence of sorbate−zeolite interaction term ($A_{sz} = 0$) at a low temperature of 200 K and sorbate concentrations of $c = 1$ and 5 *n*-butanes/α-cage, respectively. Note that in the absence of the dispersion term, curves are shifted toward the α-cage center.

TABLE 4: Relative Population of *trans* and *gauche* Forms of *n*-Butane in Zeolite NaCaA at Different Temperatures and Concentrations with and without the Presence of Sorbate−Zeolite Dispersion Interactions A_{sz}

		L-J		$A_{sz} = 0$	
T (K)	*N*	% *trans*	% *gauche*	% *trans*	% *gauche*
200	8	85.1	14.9	71.1	28.9
200	40	48.5	51.5	35.1	64.9

TABLE 5: Population of *n*-Butane Parallel ($80° \le \zeta \le 100°$) to the Inner Surface of the α-Cage in Zeolite NaCaA at Different Temperatures and Concentrations

T (K)	*N*	$80° \le \zeta \le 100°$
200	8	58.04
300	8	56.80
400	8	52.64
200	40	66.07
400	40	61.59

populations of *trans* and *gauche* are presented in Table 4 where we find that *gauche* population is enhanced when $A_{sz} = 0$. The effective volume of the cage which can be populated by *n*-butanes reduces as is evident from the resulting $\rho_{coc-com}(r)$, which is now shifted toward lower value of *r*. This is shown in Figure 9 where the curve gives $\rho_{coc-com}(r)$ for $T = 200$ K and $c = 1$ and 5 *n*-butanes/α-cage when $A_{sz} = 0$. In the case of zeolite Y, cage-to-cage migration of *n*-butanes is facile and there the *gauche* population is reduced when $A_{sz} = 0$.[28]

At $c = 1$ *n*-butane/α-cage we find that *gauche* population is lower than that found in pure fluid. We attribute the lower *gauche* population to the following: (i) The fraction of *n*-butanes that are near $\zeta = 90°$, i.e., "parallel" to the inner surface (see Figure 7) is smaller. This is evident from Table 5, which lists the proportion of *n*-butane that is within $80° \le \zeta \le 100°$ at various temperatures and sorbate concentrations. (ii) Secondly, even when they are "parallel" to the inner surface, they may be relatively far away from the inner surface of the α-cage. See Figure 3 where the peak in $\rho_{coc-com}(r)$ occurs at around 3.1 Å instead of 3.5 Å observed for $c = 5$ *n*-butanes/α-cage. When

TABLE 6: Proportion of *trans* and *gauche* *n*-Butanes among Those That Are Closely Aligned to the Inner Surface (i.e., $r_{coc-com} > r_{align}$, where r_{align} is taken as 3.2 and 3.4 Å, respectively for $c = 1$ *n*-butane/α-cage and $c = 5$ *n*-butanes/α-cage) and Those Which Are Parallel ($80° \le \zeta \le 100°$) and Those Which Are Nonparallel ($\zeta < 80°$ or $\zeta > 100°$)[a]

		overall av	$80° \le \zeta \le 100°$		$\zeta < 80°$ or $\zeta > 100°$	
T (K)	*N*	% *gauche*	% *trans*	% *gauche*	% *trans*	% *gauche*
200	8	14.9	76.1	23.9	88.5	11.5
400	8	40.4	53.5	46.5	55.2	44.8
200	40	51.5	20.7	79.3	63.4	36.6
400	40	56.7	28.0	72.0	42.3	57.7

[a] The overall average of *gauche* is also listed. Note that at low temperatures, the proportion of *gauche* is higher than average among the *n*-butanes parallel to the α-cage while it is lower than average among *n*-butanes, not parallel to the inner surface.

n-butanes are not close to the inner surface, it is not necessary that the molecular curvature match the curvature of the inner surface of the α-cage. Hence, in this situation the *n*-butane molecules can assume *trans* as well as *gauche* conformations. Further, when the *n*-butanes are not "parallel" to the inner surface, it appears that there is a preference for *trans*. Evidence for this comes from the following analysis: for the situation when the *n*-butanes are closely aligned, which is realized by imposing the condition that $r_{coc-com}$ is greater than some value r_{align}. We have chosen r_{align} equal to 3.2 Å for $c = 1$ *n*-butane/α-cage and 3.4 Å for $c = 5$ *n*-butanes/α-cage. We have then bifurcated these into those with (i) $80° \le \zeta \le 100°$ (parallel) and (ii) $\zeta < 80°$ or $\zeta > 100°$ (nonparallel). Table 6 lists the proportion of *trans* and *gauche* *n*-butanes. The results are revealing. It is evident from the table that among molecules which are closely aligned to the inner surface and parallel to it, the proportion of *gauche* conformer is significantly higher than average. Thus, for example, at 200 K and $c = 5$ *n*-butanes/α-cage, 79.3% of the *n*-butanes are *gauche* as compared to the average of only 51.5%. This result further supports the suggestion that higher *gauche* population observed at certain temperatures and sorbate concentrations may be due to the influence of the curvature of the inner surface of the α-cage. It may also be seen that at low temperatures among *n*-butanes which are close to the inner surface ($r_{coc-com} > r_{align}$) but are not parallel to it ($\zeta < 80°$ or $\zeta > 100°$), the proportion of *gauche* conformers is lower than average. Thus, for example, at $T = 200$ K and $c = 1$ *n*-butane/α-cage, 11.5% are *gauche* as compared to the average value of 14.9%. At higher temperatures, it is seen that the percentage of *gauche* population can be higher than average among nonparallel *n*-butanes. It follows from this that among *n*-butanes whose com is far removed from the inner surface of the α-cage, the population of *trans* conformer is significantly higher than average. It is not clear to us why a nonparallel *n*-butane should have a greater preference for the *trans* as compared to the pure fluid. It may be that only a *trans* can be nonparallel, presumably due to its not so low center-of-mass as compared to the *gauche*. However, the fact that *n*-butanes perpendicular to the inner surface of the α-cage prefer to have a higher *trans* conformation also explains why in zeolite Y there was no enhancement of *trans* conformer population: the surface area inside an α-cage in zeolite Y is rather small since the 12-ring windows are large, thus giving little or no *n*-butanes which are perpendicular to the inner surface.[22]

Interestingly, confined fluid exhibits more structure than the corresponding pure fluid at the same density. Figure 10 shows the *n*-butane−*n*-butane radial distribution functions (rdf) between the com, CH_3 and CH_2 groups. The increased structure

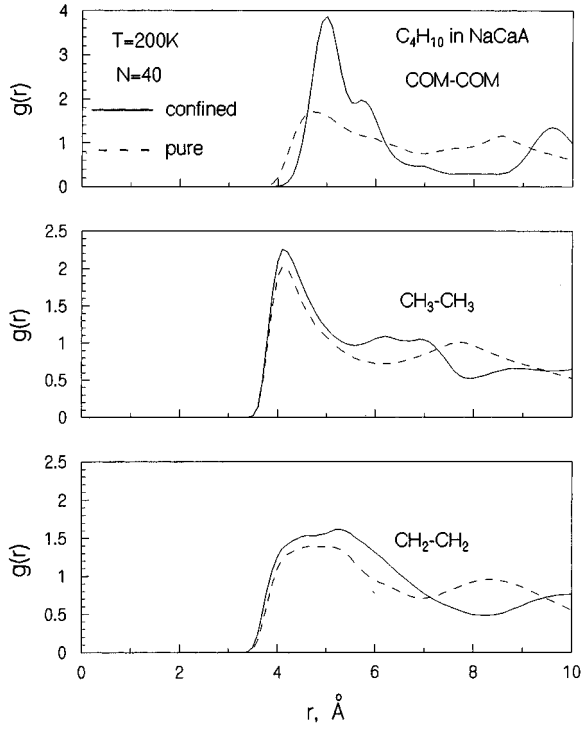

Figure 10. Sorbate−sorbate radial distribution functions $g(r)$ between the com, CH_3, and CH_2 groups of the *n*-butane molecules confined in zeolite NaCaA and those in pure fluid at the same density and temperature. It is clear from the figure that the confined *n*-butane molecules are more structured than those in pure fluid.

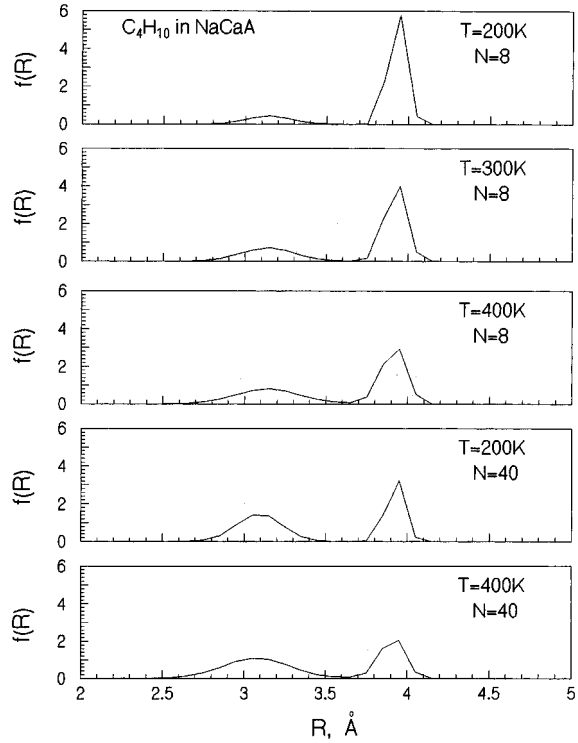

Figure 11. Distribution of end-to-end distance, R of *n*-butane molecules confined in zeolite NaCaA at different temperatures and concentrations. The curves consist of two peaks. The peak around 3.9 Å corresponds to the *trans* conformation and that around 3.1 Å corresponds to the *gauche* form.

in the rdf's may be attributed to the nonuniform potential energy surface inside the α-cage where certain regions have significantly high and unfavorable energies while other regions are associated with lower and favorable sorbate−zeolite potential energies. This leads to strong preference for certain regions inside the α-cage which in turn can give rise to more intense peaks in the rdf's. Also, the second peak in the three rdf's shown in Figure 10 for the confined fluid does not coincide with the second peak in the pure fluid. This suggests a significantly different short range order in the confined fluid as compared to the pure fluid.

3.4. Effect of Temperature on *n*-Butane Conformation. Figure 11 shows the distribution of end-to-end distance $f(R)$ of *n*-butane molecules confined in zeolite A at different temperatures and concentrations. End-to-end distance is calculated as the distance between the two end methyl groups of an *n*-butane molecule. All the curves consist of two peaks. A very sharp narrow peak of high intensity is observed corresponding to an end-to-end distance of ∼3.9 Å. A broad shoulder with much lower intensity is observed around an end-to-end distance of 3.1 Å. The end-to-end distance of a perfect *trans n*-butane molecule is 3.95 Å and that of a perfect *gauche* form is 3.11 Å. Therefore the peak around 3.9 Å corresponds to the *trans* conformation and that around 3.1 Å corresponds to the *gauche* form. The percent *gauche* population obtained by integrating the peaks in Figure 8 compares well with those obtained from Figure 2 and listed in Table 3. We have observed that the intensity at an end-to-end distance lying between the *trans* and the *gauche* form is almost zero particularly at low temperature, which is consistent with absence of any increase in intensity for intermediate values of ϕ viz., between 60 and 180° in the dihedral angle distribution discussed earlier (see Figure 2). Hernandez and Catlow[17] have observed an increase in the *gauche* population of *n*-butane in silicalite from 5.6% to 15.04% when the temperature was increased from 200 to 400 K at a sorbate concentration of 4 *n*-butanes/unit cell.

We attempt to understand the changes in *gauche* population with temperature. Firstly, we discuss changes at $c = 1$ *n*-butane/α-cage, which is about 25.5% when going from 200 to 400 K. This is marginally larger than the change in the pure fluid (23.4%) and is attributed to the depression in *gauche* population at low temperature. Note that the influence of the surface on the conformation is lower at higher temperatures since the *n*-butanes are not any more tightly bound to or aligned with the inner surface of the α-cage, and hence at sufficiently high temperature the *gauche* population in the confined fluid should approach that of the pure fluid. At $c = 5$ *n*-butanes/α-cage, the change in the *gauche* population in the confined fluid is about 5.2%, which is much smaller than what is observed in the pure fluid (31.5%). This change is smaller for the following reasons. Increase in temperature leads usually to an increase in the population of the higher energy *gauche* conformer in accordance with the Boltzmann probability. It should be noted that the energy difference between a *trans* and *gauche n*-butane in zeolite A is not equal to the difference in the $\phi_t(\phi)$ since there are additional terms. The energy of *gauche* and *trans* varies depending on the environment it is placed in, and hence this is not easy to calculate. Their energies may vary over a larger range than those in pure fluid due to the widely differing environment from one point to another within the zeolite. There is another simultaneously acting factor: with increase in temperature, *n*-butanes which were closely aligned with the inner surface of the α-cage are not any more so and hence they convert from *gauche* to *trans*. While the former leads to an increase, the latter leads to a decrease so that the net effect is little change in *gauche* population at $c = 5$ *n*-butane/α-cage concentration. This behavior is attributed to strong sorbate−sorbate interaction.

4. Conclusions

In conclusion, it appears that the *n*-butanes in zeolite A behave in unexpected manner. At low concentrations, there is a

decrease in the *gauche* population as compared to the pure fluid at the same density. At high concentrations, there is an enhancement of *gauche* population relative to the pure fluid at the same density. The reason for such an enhancement appears to be different from the reason for the enhancement of *trans* in silicalite. It is attributed to the alignment of the *n*-butane with the inner wall of the α-cage necessitating the carbon backbone of the *n*-butanes to assume the same curvature as the inner surface of the α-cage. It is suggested that *gauche* has a similar curvature as the inner surface, and hence there is an enhancement in *gauche* population. The changes in *gauche* conformer population with temperature and sorbate concentration can also be understood in terms of this. In particular, the large increase in *gauche* population at higher sorbate concentrations arises from the significant sorbate−sorbate interactions. These studies point to the inadequacy of the steric effects alone in understanding the effect of the confining medium, in the present case, zeolites on the conformation of *n*-butanes and in general alkanes. When the sorbate−zeolite dispersion term is not included between *n*-butane and the atoms of zeolite A, then we find that there is an enhancement of *gauche* conformer population. This is attributed to the shrinking of the α-cage leading to an increase in the curvature of the inner surface of the α-cage arising from the long distance tail of the sorbate−zeolite interaction. Fluid *n*-butane exhibits stronger structure when confined in zeolite A.

It would be interesting to see if experimentally one can observe similar behavior of *n*-butane sorbed in zeolite A. It would also be worthwhile to see if the variation in conformational population of *trans* and *gauche* observed here as a function of temperature and sorbate concentration is found experimentally. It should be possible to employ NMR, neutron scattering, and allied techniques to see the influence of zeolite A on the conformation of *n*-butanes. Apart from the intrinsic interest in the behavior of *n*-butane in zeolite A which such experiments will serve to satisfy, they will also indicate how realistic are the calculations such as the one presented here. Further, it will indicate the limitations, if any, of the intermolecular potentials employed here. It is necessary to take into account the effect of cations in such calculations as a recent work suggests.[29]

Acknowledgment. Authors acknowledge computational facilities provided by the Supercomputer Education and Research Centre, Indian Institute of Science, where the work has been carried out. S.B. gratefully acknowledges the Council of Scientific and Industrial Research (C.S.I.R), New Delhi, India, for the award of a fellowship. Authors acknowledge the support of the Department of Science and Technology, Government of India, for partial funding of this work. The authors gratefully acknowledge useful discussions with S. Balasubramanian on the CBMC method.

References and Notes

(1) Barrer, R. M. *Zeolites and Clay Minerals as Sorbents and Molecular Sieves;* Academic Press: New York, 1978.
(2) Breck, D. W. *Zeolite Molecular Sieves;* Wiley: New York, 1974.
(3) Karger, J.; Ruthven, D. M. *Diffusion in Zeolites;* John Wiley & Sons: New York, 1992.
(4) Heink, W.; Karger, J.; Pfeifer, H.; Salverda, P.; Datema, K. P.; Nowak, A. *J. Chem. Soc., Faraday Trans.* **1992**, *88*, 3505.
(5) Jobic, H.; Bee, M.; Kearley, G. J. *Zeolites* **1989**, *9*, 312.
(6) Jobic, H.; Bee, M.; Caro, J.; Bulow, M.; Karger, J. *J. Chem. Soc., Faraday Trans.* **1989**, *85*, 4201.
(7) Jobic, H.; Bee, M.; Kearley, G. J. *J. Phys. Chem.* **1994**, *98*, 4660.
(8) Woods, G. B.; Rowlinson, J. S. *J. Chem. Soc., Faraday Trans. 2* **1989**, *85*, 765.
(9) Yashonath, S.; Demontis, P.; Klein, M. L. *Chem. Phys. Lett.* **1988**, *153*, 551.
(10) Yashonath, S.; Demontis, P.; Klein, M. L. *J. Phys. Chem.* **1991**, *95*, 5881.
(11) Goodbody, S. J.; Watanabe, K.; MacGowan, D.; Walton, J. P. R. B.; Quirke, N. *J. Chem. Soc., Faraday Trans.* **1991**, *87*, 1951.
(12) June, R. L.; Bell, A. T.; Theodorou, D. N. *J. Phys. Chem.* **1992**, *96*, 1051.
(13) Demontis, P.; Suffritti, G. B.; Fois, E. S.; Quartieri, S. *J. Phys. Chem.* **1992**, *96*, 1482.
(14) Smit, B.; Siepmann, J. I. *J. Phys. Chem.* **1994**, *98*, 8442.
(15) Pluth, J. J.; Smith, J. V. *J. Am. Chem. Soc.* **1980**, *102*, 4704.
(16) Majinn, E. J.; Bell, A. T.; Theodorou, D. N. *J. Phys. Chem.* **1995**, *99*, 2057.
(17) Hernandez, E.; Catlow, C. R. A. *Proc. R. Soc. London, Ser. A* **1995**, *448*, 143.
(18) Van der Ploeg, P.; Berendsen, H. J. C. *J. Chem. Phys.* **1982**, *76*, 3271.
(19) Jorgensen, W. L.; Madura, J. D.; Swenson, C. J. *J. Am. Chem. Soc.* **1984**, *106*, 6638.
(20) Allen, M. P.; Tildesley, D. J. *Computer Simulation of Liquids*; Clarendon Press: Oxford, U.K., 1987.
(21) Yashonath, S.; Santikary, P. *J. Phys. Chem.* **1993**, *97*, 13778.
(22) Bandyopadhyay, S.; Yashonath, S. *J. Chem. Phys.* **1996**, *105*, 7223.
(23) Bandyopadhyay, S.; Yashonath, S. *Zeolites*, in press.
(24) June, R. L.; Bell, A. T.; Theodorou, D. N. *J. Phys. Chem.* **1990**, *94*, 1508.
(25) Yashonath, S.; Santikary, P. *Mol. Phys.* **1993**, *78*, 1.
(26) Yashonath, S.; Santikary, P. *J. Phys. Chem.* **1994**, *98*, 6368.
(27) Santikary, P.; Yashonath, S.; Ananthakrishna, G. *J. Phys. Chem.* **1992**, *96*, 1049.
(28) Bandyopadhyay, Sanjoy Ph.D. Thesis, Indian Institute of Science, Bangalore, India, 1996.
(29) Auerbach, S. M.; Metiu, H. I. Preprint.